J. Fluid Mech. (1990), *vol.* 219, *pp.* 337–360
Printed in Great Britain

The long-wave instability in heated or cooled inclined liquid layers

By MARC K. SMITH

Department of Mechanical Engineering, The Johns Hopkins University, Baltimore, MD 21218, USA

(Received 25 October 1988 and in revised form 5 March 1990)

A thin liquid layer flowing down an inclined plane exhibits a long-wave interfacial instability at a critical value of the Reynolds number. Past work on this problem has shown that heating or cooling the layer does not significantly change the characteristics of this instability. We show that this is not correct when the Prandtl number of the liquid is large and that both heating and cooling from below can destabilize the layer depending on the interfacial heat-transfer conditions. The mechanism for this unstable behaviour involves the direct expansion of the liquid as it experiences a temperature perturbation produced by the deformation of the interface. When the layer is heated from below, this additional effect changes the critical angle at which longitudinal, buoyancy-driven rolls are preferred relative to the long-wave interfacial instability.

1. Introduction

A thin liquid layer flowing down a rigid inclined plane is an appropriate model for a large number of technologically important processes. The theoretical work of Benjamin (1957) and Yih (1963) clearly showed that the interface of an isothermal inclined liquid layer is unstable to long-wavelength disturbances if the Reynolds number is large enough. The research on this instability and its behaviour in many related systems has since become quite extensive.

Since thin liquid layers are seen in a large number of cooling and condensation processes, a natural extension of this work is to include the effects of heat and mass transfer on the instability of the layer. The thermal effects of condensation have been examined by Bankoff (1971), Marschall & Lee (1973), Lin (1975) and Ünsal & Thomas (1978) through a modification of the normal-stress boundary condition at the interface. In a layer heated from below, Roca (1966) included buoyancy normal to the layer. Lin (1975) and Sreenivasan & Lin (1978) added the effects of a temperature-dependent surface tension, but neglected buoyancy completely. Kelly & Goussis (1982) considered buoyancy in both the normal and the longitudinal directions. Finally, the effect of a temperature-dependent viscosity was considered by Goussis & Kelly (1985).

In this paper, we shall consider the effect of heating or cooling the layer on the stability of the interface to long waves. We shall include buoyancy forces in both the longitudinal and the normal directions and also the full effect of liquid expansion. When Kelly & Goussis (1982) considered this problem, they showed that buoyancy forces and direct liquid expansion could be neglected within the layer when the thermal expansion coefficient is small. Since this is usually the case, they concluded that thermal effects do not significantly influence the characteristics of the long-wave instability in inclined layers. We shall show, however, that this result is only strictly true for a liquid layer with small to moderate values of the Prandtl number.

Heating or cooling an inclined liquid layer will significantly alter the onset of the interfacial long-wave instability when the Prandtl number of the liquid layer is large enough. The mechanism for this unstable behaviour is the direct expansion of the liquid. When the interface of the layer is deformed, advective motions in the liquid produce a temperature perturbation that causes the liquid to expand or contract in a way that increases the interfacial deformation. This temperature perturbation is proportional to the Prandtl number, and so as the Prandtl number increases its influence on the onset of the instability becomes larger.

The importance of thermal effects on the long-wave instability can be seen in two ways. First, when a layer has a nearly insulated interface and is cooled from below, it is actually less stable to long-wave disturbances than either an isothermal or a heated layer. Secondly, heating the layer from below will alter the critical angle of inclination at which longitudinal, buoyancy-driven rolls are preferred compared to transverse interfacial long waves. Both of these behaviours shall be documented in this work.

In §2, we shall define the model of a film flow down an inclined plane that is cooled or heated from below. The essential results of the long-wave stability calculation are then presented in §3. Numerical calculations for finite wavelengths are given in §4. These results demonstrate that a disturbance with a zero or a very small wavenumber is the preferred mode of long-wave instability. We then describe in §5 the physical mechanisms involved in the instability and show how they are supported by the mathematical analysis. Finally, in §6, we state our conclusions and comment on related work.

2. Mathematical analysis

The inclined liquid layer model is shown in figure 1. It is composed of a liquid layer of thickness d bounded below by a rigid plane and above by a passive gas. The rigid plane is inclined at the angle β with respect to the horizontal and gravity acts vertically downward. The bottom surface of the layer is maintained at the temperature T_b^* while the top surface undergoes convective heat transfer to the passive gas, which is held at the ambient temperature T_a^*. For purposes of scaling, the as yet unknown temperature of the top surface is T_t^*. The liquid is a Newtonian fluid in which the density is the only temperature-dependent material property. The density ρ^* has the equation of state $\rho^* = \rho_b\{1-\gamma(T^*-T_b^*)\}$, where ρ_b is the density at the temperature T_b^* and γ is the thermal expansion coefficient. The other fluid properties are the viscosity μ, kinematic viscosity $\nu = \mu/\rho_b$, thermal conductivity k, specific heat c_p, thermal diffusivity $\kappa = k/(\rho_b c_p)$, surface heat-transfer coefficient h_g, and surface tension σ. We use a coordinate system that has its origin embedded in the rigid plane with the x-axis parallel to the plane and the y-axis normal to it. The velocity, length, time and pressure are scaled with $U_s = g\sin(\beta)\,d^2/\nu, d, d/U_s$ and $\mu U_s/d$ respectively. The temperature is referred to the temperature of the bottom surface T_b^* and scaled with $\Delta T = T_t^* - T_b^*$. The dimensionless governing equations and boundary conditions for two-dimensional flow are given as follows:

$$\rho R\{u_t + uu_x + vu_y\} = -p_x + \rho + \nabla^2 u, \tag{2.1a}$$

$$\rho R\{v_t + uv_x + vv_y\} = -p_y - \cot(\beta)\rho + \nabla^2 v, \tag{2.1b}$$

$$\rho Pe\{T_t + uT_x + vT_y\} = \nabla^2 T, \tag{2.1c}$$

$$\rho_t + u\rho_x + v\rho_y + \rho(u_x + v_y) = 0, \tag{2.1d}$$

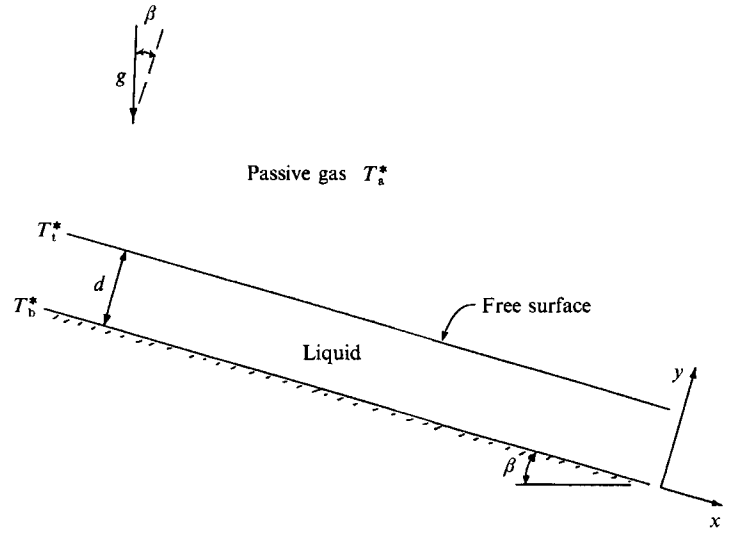

FIGURE 1. The geometry of a liquid layer on a rigid inclined plane. The layer is heated or cooled from below. The top surface is stress-free and undergoes convective heat transfer to the bounding ambient gas.

$$\rho = 1 - ET, \tag{2.1e}$$

$$u = v = T = 0 \quad \text{on} \quad y = 0, \tag{2.1f}$$

$$\left.\begin{aligned} \sigma_{ij} n_j = Ca^{-1} \mathscr{K} n_i, \quad v = \eta_t + u\eta_x \\ \nabla T \cdot \boldsymbol{n} + B(T - T_a) = 0 \end{aligned}\right\} \text{ on, } y = 1 + \eta. \tag{2.1g, h, i}$$

Here,

$$\sigma_{ij} = -p\delta_{ij} + u_{i,j} + u_{j,i}, \quad \mathscr{K} = \eta_{xx} N^{-3}, \tag{2.1j, k}$$

$$\boldsymbol{n} = (-\eta_x, 1) N^{-1}, \quad N = (1 + \eta_x^2)^{\frac{1}{2}}, \tag{2.1l, m}$$

T_a is the dimensionless temperature of the ambient passive gas, $\mathscr{K}$ is the curvature of the interface, δ_{ij} is the Kronecker delta, and lower-case letter subscripts refer to partial differentiation, except for i and j which are indices used in a standard indicial notation. Note that we do not assume that the liquid is incompressible and so we use the full form of the mass conservation equation.

The dimensionless groups that appear in these equations are the Reynolds number $R = g \sin(\beta) d^3/\nu^2$, the Péclet number $Pe = g \sin(\beta) d^3/\nu\kappa$, the expansion number $E = \gamma \Delta T$, the capillary number $Ca = \rho_b g \sin(\beta) d^2/\sigma$, and the Biot number $B = h_g d/k$. Note that $Pe = RPr$, where $Pr = \nu/\kappa$ is the Prandtl number.

The expansion number E is generally very small and so the Boussinesq approximation is usually employed to simplify the above equations. In this approximation, we would ignore all $O(E)$ terms except for the gravitational body-force terms in the momentum equations (2.1*a*, *b*). However, the scaling of this problem shows that even these terms can be ignored if temperature effects are $O(1)$. Thus, the temperature field decouples from the velocity field and we regain the result of Kelly & Goussis (1982) that thermal effects do not influence the long-wave instability of the layer. In the present work, we wish to show how thermal effects can influence the instability and so we do not make the Boussinesq approximation. Our results show that some $O(E)$ terms are multiplied by the Prandtl number and they become important if the Prandtl number is large. To simplify the presentation of the following analysis, small $O(E)$ terms are neglected, as noted, and only those terms

that produce an $O(EPr)$ effect are retained. A final result that includes all of the neglected terms up to $O(E^2)$ is also reported.

The basic state is a simple parallel shear flow, defined as

$$\bar{u} = y - \tfrac{1}{2}y^2 + \tfrac{1}{2}E\{\tfrac{1}{3}y^3 - y\}, \tag{2.2a}$$

$$\bar{p} = \cot(\beta)\{1 - y + \tfrac{1}{2}E(y^2 - 1)\}, \tag{2.2b}$$

$$\bar{v} = \bar{\eta} = 0, \tag{2.2c, d}$$

$$\bar{T} = y, \quad \bar{\rho} = 1 - Ey, \tag{2.2e, f}$$

$$T_a = 1 + B^{-1}. \tag{2.2g}$$

All $O(E)$ terms in this basic state are small compared with one and can be neglected. If we consider the dimensional ambient temperature fixed, then equation (2.2g) determines the dimensional temperature of the top surface T_t^* used in the scaling analysis.

Next, we perform a standard linear stability analysis and solve the resulting disturbance equations using normal modes defined as

$$(u', v', p', T', \rho', \eta') = (\hat{u}, \hat{v}, \hat{p}, \hat{T}, \hat{\rho}, \hat{\eta}) \exp\{i\alpha(x - ct)\}. \tag{2.3}$$

Here, α is the wavenumber of the disturbance, c is a complex eigenvalue whose real part, c_r, is the phase speed, and whose imaginary part times α, αc_i, is the growth rate of the instability. Using $\hat{\rho} = -E\hat{T}$, the final normal-mode disturbance equations are

$$\bar{\rho}R\{i\alpha(\bar{u} - c)\hat{u} + \bar{u}'\hat{v}\} = -i\alpha\hat{p} - E\hat{T} + D^2\hat{u} - \alpha^2\hat{u}, \tag{2.4a}$$

$$i\alpha\bar{\rho}R(\bar{u} - c)\hat{v} = -D\hat{p} + E\cot(\beta)\hat{T} + D^2\hat{v} - \alpha^2\hat{v}, \tag{2.4b}$$

$$\bar{\rho}Pe\{i\alpha(\bar{u} - c)\hat{T} + \bar{T}'\hat{v}\} = D^2\hat{T} - \alpha^2\hat{T}, \tag{2.4c}$$

$$-E\{i\alpha(\bar{u} - c)\hat{T} + \bar{T}'\hat{v}\} + \bar{\rho}(i\alpha\hat{u} + D\hat{v}) = 0, \tag{2.4d}$$

$$\hat{u} = \hat{v} = \hat{T} = 0 \quad \text{on} \quad y = 0, \tag{2.4e}$$

$$\left.\begin{aligned} -\hat{p} + 2D\hat{v} &= \bar{p}'\hat{\eta} - Ca^{-1}\alpha^2\hat{\eta} && (2.4f)\\ D\hat{u} + i\alpha\hat{v} &= -\bar{u}''\hat{\eta} && (2.4g)\\ \hat{v} &= i\alpha(\bar{u}(1) - c)\hat{\eta}, \quad D\hat{T} + B\hat{T} = -B\bar{T}'\hat{\eta} && (2.4h, i) \end{aligned}\right\} \quad \text{on} \quad y = 1.$$

Here, $D^j \equiv d^j/dy^j$ for $j = 1, 2$ and primes on the basic-state quantities also denote differentiation with respect to y.

These normal-mode disturbance equations are examined for long waves using a regular perturbation expansion for $\alpha \to 0$. This technique was first used by Yih (1963) for the isothermal problem. The appropriate long-wave expansions are

$$\hat{u} = u_0 + \alpha u_1 + \alpha^2 u_2 + \ldots, \quad \hat{v} = \alpha v_1 + \alpha^2 v_2 + \ldots, \tag{2.5a, b}$$

$$\hat{p} = p_0 + \alpha p_1 + \alpha^2 p_2 + \ldots, \quad \hat{T} = T_0 + \alpha T_1 + \alpha^2 T_2 + \ldots, \tag{2.5c, d}$$

$$\hat{\eta} = \eta_0 + \alpha\eta_1 + \alpha^2\eta_2 + \ldots, \quad c = c_0 + \alpha c_1 + \alpha^2 c_2 + \ldots. \tag{2.5e, f}$$

We shall use the normalization $\eta_0 = 1, \eta_j = 0, j = 1, 2, 3 \ldots$.

Implementing the regular perturbation method, we obtain the following ordered problems and their solutions. At $O(1)$ we have

$$D^2T_0 = 0, \quad T_0(0) = 0, \quad DT_0(1) + BT_0(1) = -B, \tag{2.6a, b, c}$$

$$D^2u_0 = ET_0, \quad u_0(0) = 0, \quad Du_0(1) = 1 - E, \tag{2.6d, e, f}$$

$$Dp_0 = E\cot(\beta)T_0, \quad p_0(1) = \cot(\beta)\{1 - E\}. \tag{2.6g, h}$$

All $O(E)$ terms in these equations are small compared with one and so they can be safely ignored. The solutions are

$$T_0(y) = -\mathscr{B}y, \quad u_0(y) = y, \quad p_0(y) = \cot(\beta), \tag{2.7a, b, c}$$

where $\mathscr{B} = B/(B+1)$.

At $O(\alpha)$ we have

$$\mathrm{D}v_1 = -\mathrm{i}u_0 + E\bar{\rho}^{-1}\{\mathrm{i}(\bar{u}-c_0)\,T_0 + \bar{T}'v_1\}, \tag{2.8a}$$

$$v_1(0) = 0, \quad c_0 = \bar{u}(1) + \mathrm{i}v_1(1), \tag{2.8b, c}$$

$$\mathrm{D}^2T_1 = \bar{\rho}Pe\{\mathrm{i}(\bar{u}-c_0)\,T_0 + \bar{T}'v_1\}, \tag{2.8d}$$

$$T_1(0) = 0, \quad \mathrm{D}T_1(1) + BT_1(1) = 0, \tag{2.8e, f}$$

$$\mathrm{D}^2u_1 = \mathrm{i}p_0 + ET_1 + \bar{\rho}R\{\mathrm{i}(\bar{u}-c_0)\,u_0 + \bar{u}'v_1\}, \tag{2.8g}$$

$$u_1(0) = 0, \quad \mathrm{D}u_1(1) = 0. \tag{2.8h, i}$$

In the solution of these equations, we can ignore all $O(E)$ terms except for the ET_1 term in (2.8g) because T_1 is of $O(Pr)$ and we wish to retain terms of $O(EPr)$. This $O(E)$ term represents the effect of buoyancy in the longitudinal direction that is introduced through the advection of heat described by (2.8d). The solutions for these equations are

$$v_1(y) = -\mathrm{i}\tfrac{1}{2}y^2, \quad c_0 = 1, \tag{2.9a, b}$$

$$T_1(y) = \mathrm{i}Pe\left\{-\frac{y^4}{24} + \frac{y}{6} + \mathscr{B}\left(\frac{y^5}{40} - \frac{y^4}{12} + \frac{y^3}{6} - \frac{5y}{12}\right) + \mathscr{B}^2\frac{11y}{60}\right\}, \tag{2.9c}$$

$$u_1(y) = \mathrm{i}R\left\{\frac{y^4}{24} - \frac{y^3}{6} + \frac{y}{3}\right\} + \mathrm{i}\cot(\beta)\left\{\frac{y^2}{2} - y\right\}$$
$$+ \mathrm{i}EPe\left\{-\frac{y^6}{720} + \frac{y^3}{36} - \frac{3y}{40} + \mathscr{B}\left(\frac{y^7}{1680} - \frac{y^6}{360} + \frac{y^5}{120} - \frac{5y^3}{72} + \frac{43y}{240}\right) + \mathscr{B}^2\left(\frac{11y^3}{360} - \frac{11y}{120}\right)\right\}. \tag{2.9d}$$

Finally, at $O(\alpha^2)$ we have

$$\mathrm{D}v_2 = -\mathrm{i}u_1 + E\bar{\rho}^{-1}\{\mathrm{i}(\bar{u}-c_0)\,T_1 - \mathrm{i}c_1T_0 + \bar{T}'v_2\}, \tag{2.10a}$$

$$v_2(0) = 0, \quad c_1 = \mathrm{i}v_2(1). \tag{2.10b, c}$$

When $O(E)$ terms are ignored in this differential equation, but terms of $O(EPr)$ retained, (2.10a) becomes

$$\mathrm{D}v_2 = -\mathrm{i}u_1 + E\mathrm{i}(\bar{u}-c_0)\,T_1. \tag{2.10d}$$

The solution is

$$v_2(y) = R\left\{\frac{y^5}{120} - \frac{y^4}{24} + \frac{y^2}{6}\right\} + \cot(\beta)\left\{\frac{y^3}{6} - \frac{y^2}{2}\right\} + EPe\left\{-\frac{y^7}{315} + \frac{y^6}{144} - \frac{y^5}{120} + \frac{y^4}{36} - \frac{y^3}{18} + \frac{11y^2}{240}\right.$$
$$\left. + \mathscr{B}\left(\frac{11y^8}{6720} - \frac{5y^7}{504} + \frac{y^6}{30} - \frac{y^5}{20} - \frac{y^4}{36} + \frac{5y^3}{36} - \frac{19y^2}{160}\right) + \mathscr{B}^2\left(\frac{11y^4}{360} - \frac{11y^3}{180} + \frac{11y^2}{240}\right)\right\}, \tag{2.11a}$$

$$c_1 = i\left\{\frac{2}{15}R - \frac{1}{3}\cot(\beta) + EPe\left(\frac{17}{1260} - \frac{73}{2240}\mathscr{B} + \frac{11}{720}\mathscr{B}^2\right)\right\}. \tag{2.11b}$$

When c_i is positive, the system is unstable. Setting $c_i = 0$ and using the relation $Pe = RPr$, we obtain the critical Reynolds number

$$R_c = \tfrac{5}{2}\cot(\beta)\left\{1 + EPr\left(\frac{17}{168} - \frac{219}{896}\mathscr{B} + \frac{11}{96}\mathscr{B}^2\right)\right\}^{-1}. \tag{2.12a}$$

For an insulated top surface ($\mathscr{B} = 0$)

$$R_c = \tfrac{5}{2}\cot(\beta)\left\{1+\frac{17}{168}EPr\right\}^{-1}, \tag{2.12b}$$

and for an isothermal top surface ($\mathscr{B} = 1$)

$$R_c = \tfrac{5}{2}\cot(\beta)\left\{1-\frac{11}{384}EPr\right\}^{-1}. \tag{2.12c}$$

When $E = 0$, we regain the result obtained by Benjamin (1957) and Yih (1963) for an isothermal layer when the difference in the velocity scale is considered.

We neglected the small $O(E)$ terms in the above analysis in order to emphasize our main result concerning the importance of $O(EPr)$ terms. When these terms are included, we obtain

$$c_0 = 1+E\left(-\frac{2}{3}-\frac{1}{12}\mathscr{B}\right)+E^2\left(-\frac{1}{60}\mathscr{B}+\frac{1}{24}\mathscr{B}^2\right)+O(E^3), \tag{2.13a}$$

$$\begin{aligned} c_1 = \mathrm{i}\Bigg\{&\frac{2}{15}R-\frac{1}{3}\cot(\beta)+E\Bigg[R\left(-\frac{671}{2520}-\frac{799}{20160}\mathscr{B}\right)\\ &+\cot(\beta)\left(\frac{5}{24}+\frac{3}{40}\mathscr{B}\right)+Pe\left(\frac{17}{1260}-\frac{73}{2240}\mathscr{B}+\frac{11}{720}\mathscr{B}^2\right)\Bigg]\\ &+E^2\Bigg[R\left(\frac{715}{4032}+\frac{61}{1344}\mathscr{B}+\frac{2761}{120960}\mathscr{B}^2\right)+\cot(\beta)\left(\frac{19}{720}\mathscr{B}-\frac{3}{80}\mathscr{B}^2\right)\\ &+Pe\left(-\frac{71}{4032}+\frac{1427}{60480}\mathscr{B}+\frac{1207}{67200}\mathscr{B}^2-\frac{19}{1080}\mathscr{B}^3\right)\Bigg]\Bigg\}+O(E^3). \end{aligned} \tag{2.13b}$$

From this, the critical Reynolds number is

$$R_c = \tfrac{5}{2}\cot(\beta)f_n/f_d, \tag{2.13c}$$

where

$$f_n = 1+E\left(-\frac{5}{8}-\frac{9}{40}\mathscr{B}\right)+E^2\left(-\frac{19}{240}\mathscr{B}+\frac{9}{80}\mathscr{B}^2\right)+O(E^3), \tag{2.13d}$$

$$\begin{aligned} f_d = 1&+E\left(-\frac{671}{336}-\frac{799}{2688}\mathscr{B}+Pr\left[\frac{17}{168}-\frac{219}{896}\mathscr{B}+\frac{11}{96}\mathscr{B}^2\right]\right)\\ &+E^2\left(\frac{3575}{2688}+\frac{305}{896}\mathscr{B}+\frac{2761}{16128}\mathscr{B}^2+Pr\left[-\frac{355}{2688}+\frac{1427}{8064}\mathscr{B}+\frac{1207}{8960}\mathscr{B}^2-\frac{19}{144}\mathscr{B}^3\right]\right)+O(E^3). \end{aligned} \tag{2.13e}$$

The simpler results in (2.9*b*), (2.11*b*) and (2.12*a*) can be recovered from the results shown in (2.13) by retaining the $O(EPr)$ terms and neglecting all other $O(E)$ terms. This result verifies the correctness of the simpler analysis.

3. Long-wave results

When $Pr = O(1)$, the critical Reynolds number, from (2.13*c*), is

$$R_c = \tfrac{5}{2}\cot(\beta)+O(E). \tag{3.1}$$

This clearly shows that thermal effects produce only small changes in the critical Reynolds number compared to the isothermal value. This is the result of Kelly &

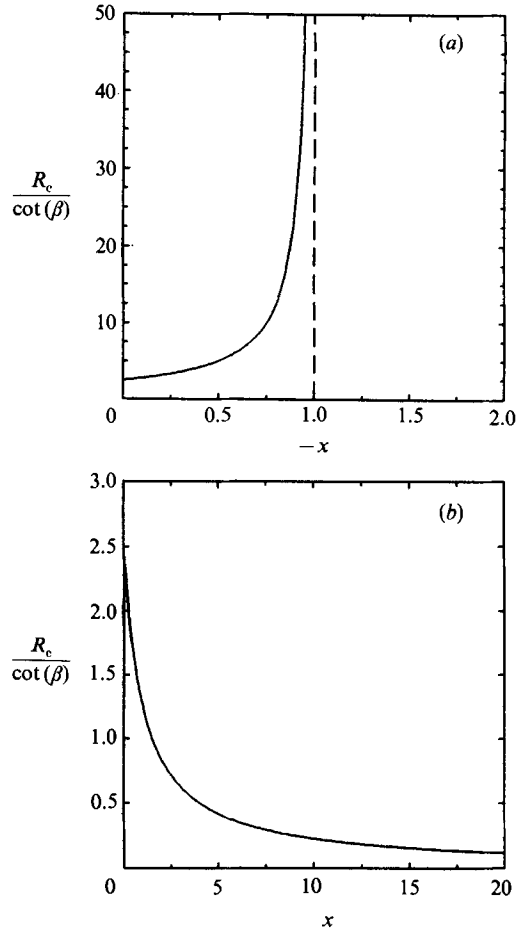

FIGURE 2. The behaviour of the critical Reynolds number R_c for long waves versus the polynomial function x, defined by (3.2).

Goussis (1982). However, when $EPr = O(1)$, thermal effects have a pronounced effect on the critical Reynolds number as shown in (2.12a). Rewriting (2.12a) as

$$R_c = \tfrac{5}{2}\cot(\beta)(1+x)^{-1}, \tag{3.2a}$$

$$x = EPr\left(\frac{17}{168} - \frac{219}{896}\mathscr{B} + \frac{11}{96}\mathscr{B}^2\right), \tag{3.2b}$$

we see that the critical Reynolds number behaves as shown in figure 2.For negative values of x, R_c increases as x decreases, showing that the layer is stabilized by the thermal conditions. For $x < -1$, the layer is completely stabilized to long waves. For positive values of x, R_c monotonically decreases as x increases. Thus, the layer is destabilized by the thermal conditions.

The sign of x determines the behaviour of the liquid layer to thermal effects. Positive values of E indicate a layer cooled from below, while negative values are for a layer heated from below. We also note that the polynomial expressed as x monotonically decreases with $\mathscr{B}$ for $\mathscr{B} \in (0, 1)$. When $\mathscr{B} = 0$ (insulating), $x = EPr\,17/168$, and when $\mathscr{B} = 1$ (isothermal), $x = -EPr\,11/384$. The crossover point is

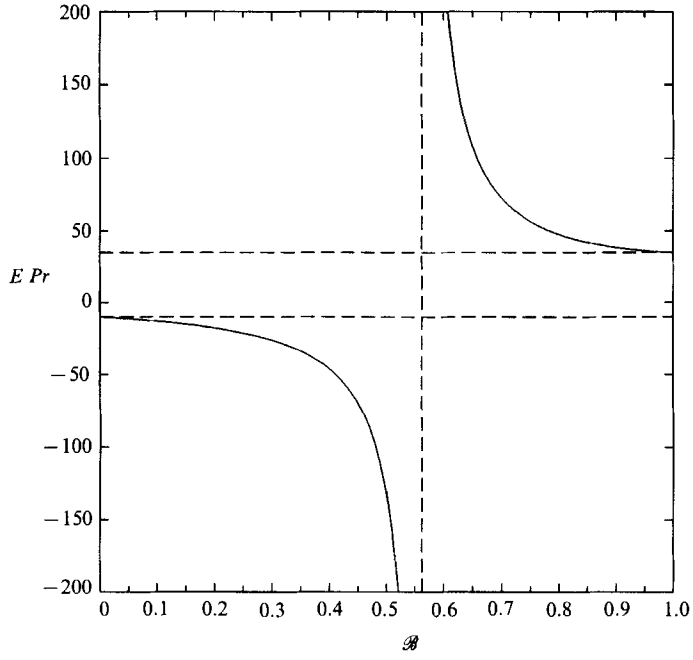

FIGURE 3. The value of EPr at which complete stabilization of the interface to long waves occurs versus the parameter $\mathscr{B}$.

$\mathscr{B} = 0.562$, which is the Biot number $B = 1.28$. Thus, the layer behaves as follows. When the top surface is approximately isothermal ($B > 1.28$), heating destabilizes the layer and cooling stabilizes it. This is the behaviour consistent with our understanding of Rayleigh–Bénard convection in a horizontal layer. However, when the top surface is approximately insulating ($B < 1.28$), cooling destabilizes the layer and heating stabilizes it. This is unexpected and indicates an instability mechanism somewhat different from previous experience.

Figure 2(a) shows that enough heating or cooling can completely stabilize a liquid layer to long waves with zero wavenumber. This occurs when $x < -1$, from which we produce figure 3. The inequality corresponds to the regions in the upper right and lower left corners of the figure. This figure shows that a layer with an approximately isothermal top surface ($0.562 < \mathscr{B} < 1$) is completely stabilized to long waves for a large enough cooling from below. In a layer with an approximately insulating top surface ($0 < \mathscr{B} < 0.562$), a large enough heating from below will completely stabilize the layer to long waves. The extremal points of these curves are $EPr = 34.91$ for an isothermal top surface ($\mathscr{B} = 1$), and $EPr = -9.882$ for an insulated top surface ($\mathscr{B} = 0$).

When the liquid layer is on a vertical surface, (2.11b) reduces to

$$c_1 = \mathrm{i}R_{15}^{2}(1+x), \tag{3.3}$$

where x is given by (3.2b). The vertical layer is stable if $x < -1$. Thus, figure 3 also gives the critical value of heating or cooling (depending on the thermal conditions of the top surface) for complete stabilization of a vertical layer to long waves.

We can isolate the thermal effects seen in the long-wave instability by noting that

as $Pr \to \infty, R \to 0$. In this limit, the fluid flow in the layer is completely viscous, but an instability still exists since Pe approaches a constant. We find

$$E\,Pe_c = 20\cot(\beta)\left\{\frac{17}{21} - \frac{219}{112}\mathscr{B} + \frac{11}{12}\mathscr{B}^2\right\}^{-1}. \tag{3.4}$$

An isothermal upper surface ($\mathscr{B} = 1$) yields $E\,Pe_c = -\cot(\beta)\,960/11$. This indicates that the instability occurs when the layer is heated from below. For an insulated upper surface ($\mathscr{B} = 0$), we obtain $E\,Pe_c = \cot(\beta)\,420/17$. Thus, unstable long waves are possible when the layer is cooled from below.

4. Finite-wavelength results

The long-wavelength, surface-wave instability of an inclined, isothermal liquid layer occurs at a critical wavenumber of $\alpha = 0$. This has been confirmed by DeBruin (1974) and Floryan, Davis & Kelly (1987) who showed numerically that the neutral curve corresponding to the interfacial mode has a global minimum in Reynolds number at $\alpha = 0$. They also showed that the shear mode of instability associated with this flow occurs at a higher value of the Reynolds number except when the angle of inclination is extremely small, i.e. less than half a minute of arc. Thus, the interfacial long-wave instability is preferred for all but the smallest inclination angles.

In the stability analysis of the previous section, we showed that it is possible for the liquid layer to be completely stabilized to long waves under specific sets of thermal conditions. Under these conditions, it is possible that the critical value of the Reynolds number for surface waves occurs at a non-zero value of the wavenumber. To determine if this is so, we solved the normal-mode stability equations (2.4) numerically using SUPORT, a code written by Scott & Watts (1975, 1977). This code uses Runge–Kutta integration and a superposition technique to solve two-point boundary-value problems. Orthonormalization is employed to accurately calculate the solution when the problem is stiff. Iteration routines using the secant method were written by the author to perform the iteration on the eigenvalue and to find the neutral point. Successful checks of the numerical solution with the numerical results of Floryan *et al.* (1987), with the long-wave approximations given by (2.13), and with the results of the associated adjoint eigenvalue problem provided confidence that the equations were correctly coded and solved.

The neutral curves of Reynolds number versus wavenumber are functions of Ca, β, B, E and Pr. The capillary number represents the effect of surface tension that tends to stabilize the interface. For long waves, its effect is negligible as shown by the fact that this parameter does not appear in the long-wave results of the previous section. Thus, we shall set the surface tension to zero, i.e. $Ca^{-1} = 0$, in the numerical calculations. The cotangent of the angle of inclination β has a scalar effect on the critical Reynolds number for long waves. For simplicity, we set $\beta = 45°$ in our computations.

Our ultimate goal in this work is to explore the effect of the Prandtl number on the interfacial instability subject to specific thermal conditions in the layer. So, we shall consider a cooled liquid layer with the expansion number $E = 10^{-3}$ and a heated layer with $E = -10^{-3}$. For an isothermal top surface, we set the Biot number $B = \infty$ and for an insulated surface, $B = 0$.

The numerical calculation of a point on a neutral curve for large values of the

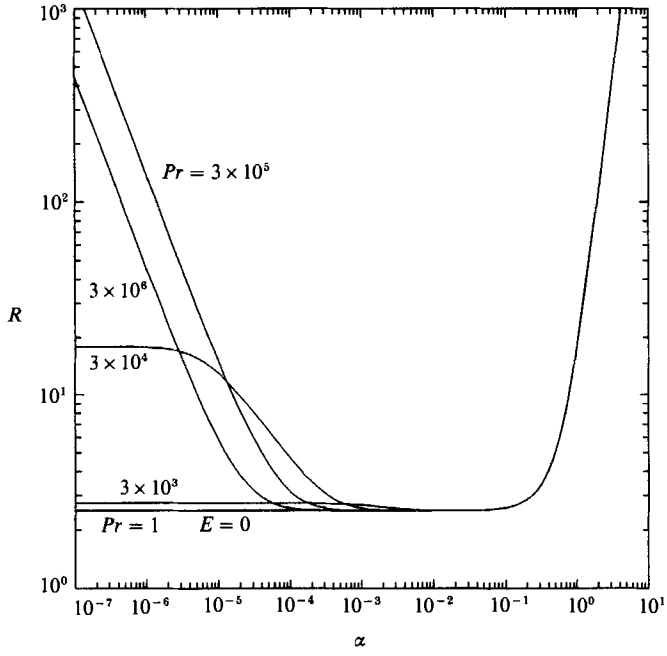

FIGURE 4. Neutral curves of the Reynolds number R versus the wavenumber α for different values of the Prandtl number Pr. The system is stable below the curves and unstable above. The layer is cooled from below and has an isothermal top surface. Other parameter values are $E = 10^{-3}$, $B = \infty$, $Ca = \infty$ and $\beta = 45°$. The neutral curve for the isothermal case $E = 0$ is also shown, but it is indistinguishable from the curve for $Pr = 1$ because they differ by only an $O(E)$ amount.

Prandtl number and 'large' enough values of the wavenumber fails owing to either orthonormalization problems or because it is extremely time consuming. However, figures 4, 5, 7 and 8 show that the neutral curves for large values of the Prandtl number become indistinguishable on this scale from the neutral curve for $Pr = 1$ well before the failure in the calculation occurs. For example, the calculation for $Pr = 3 \times 10^6$ in figure 4 was stopped because of time at $\alpha = 0.005$. Thus, even though we could not calculate the complete neutral curve up to $\alpha = 1$ or higher for the larger values of the Prandtl number, we feel that all of these neutral curves are actually indistinguishable from the $Pr = 1$ neutral curve for 'large' values of the wavenumber as suggested by the figures.

We can verify this supposition for a layer with an isothermal top surface by noting that a good approximation to the temperature field in the limit of $Pr \to \infty$ can be found by solving the energy equation (2.4c). The result is

$$\hat{T} = -\bar{T}'\hat{v}/\mathrm{i}\alpha(\bar{u}-c), \tag{4.1}$$

which also satisfies the boundary conditions at the top and the bottom surfaces. This temperature field is then used in the solution of the momentum and continuity equations to obtain a neutral curve for the large-Prandtl-number limit. This approximate neutral curve should be accurate for the larger values of the wavenumber and it is relatively easy to compute all the way to $\alpha = 1$. It differs from the neutral curve for $Pr = 1$ by only an $O(E)$ amount and so the two curves are indistinguishable in figures 4 and 5. All the neutral curves for large Prandtl numbers in the two layers with an isothermal top surface merge with this curve as α becomes 'large'.

Pr	1.0×10^2	2.0×10^2	1.0×10^3	3.0×10^3	3.0×10^4	3.0×10^5	3.0×10^6
R_c	2.5108	2.5170	2.5124	2.5086	2.5051	2.5039	2.5036
α_c	0.000	0.018	0.023	0.017	0.010	0.006	0.003

TABLE 1. The critical Reynolds number R_c and the critical wavenumber α_c for various values of the Prandtl number Pr corresponding to figure 4. The layer is cooled from below and has an isothermal top surface. Other parameter values are $E = 10^{-3}$, $B = \infty$, $Ca = \infty$ and $\beta = 45°$.

The neutral curves for a cooled layer with an isothermal surface ($E = 10^{-3}$ and $B = \infty$) are shown in figure 4 for various values of the Prandtl number. First, for $Pr = 1$ we see that the system has a preferred long-wave instability because the neutral curve has a minimum at $\alpha = 0$ and monotonically increases as α increases. We also see that the neutral curve for the isothermal layer is indistinguishable from the $Pr = 1$ neutral curve because the two differ by only an $O(E)$ amount. As the Prandtl number is increased, the long-wave stabilization is clearly evident. For this value of E, the complete long-wave stabilization occurs for $Pr > 35000$. This is shown in the two curves for $Pr = 3\times10^5$ and 3×10^6. For these two curves, we find that R behaves like α^{-1} as $\alpha\to0$. The critical points of these neutral curves are shown in table 1. Here we see that the critical Reynolds numbers differ from the isothermal value of 2.5 by only an $O(E)$ amount. Thus, the onset of instability in this case is essentially governed by the isothermal layer.

The neutral curves for a heated layer with an isothermal surface ($E = -10^{-3}$ and $B = \infty$) are shown in figure 5. The destabilizing effect of heating is clearly evident. Thus, the long-wave results of the previous section do predict the critical value of the Reynolds number for heating. Note that the thermal effects are confined to wavenumbers of less than 10^{-4}. The region of influence of these thermal effects can be clearly seen by considering the limit of $Pr\to\infty$, in which $R_c\to0$ and $R_c Pr = Pe_c$ approaches a constant. The neutral curves for this limit and for three values of E are shown in figure 6. When plotted as $-EPe$ versus $-\alpha/E$ all the neutral curves collapse onto the single curve shown in the figure. Since the expansion number is generally small, we see that the region of influence of the thermal effects on the long-wave instability is confined to wavenumbers of $O(E)$. This extreme localization was also seen for the case of cooling. Note that in this limit of $Pr = \infty$, the neutral curves represent an instability due to thermal effects alone. Inertial effects, which cause the instability of the isothermal liquid layer, are completely negligible.

Now, consider a layer with an insulating top surface. The neutral curves for cooling ($E = 10^{-3}$ and $B = 0$) are shown in figure 7. Here we see the long-wave destabilization predicted by our perturbation analysis. The extent of the influence of the thermal effects is the same as for the heated layer with an isothermal top surface, as shown in figure 5. However, the neutral curves behave very differently near $R = 2.5$. For the heated layer, the lower part of the neutral curve representing the thermal mode is smoothly connected to the upper part of the curve representing the inertial mode for all finite values of Pr that we examined. When $Pr = \infty$, we see only a single curve for the thermal mode as shown in figure 6. In figure 7, when Pr is large enough, we see two distinct branches of the neutral curve; a lower branch for the thermal mode and an upper branch for the inertial mode. For Pr just above 3×10^5, the two branches merge to form one continuous curve.

The neutral curves for a heated layer with an insulating top surface ($E = -10^{-3}$ and $B = 0$) are shown in figure 8. The long-wave stabilization we predicted is evident in the curve for $Pr = 8000$. When $Pr = 8\times10^4$, there is no long-wave instability;

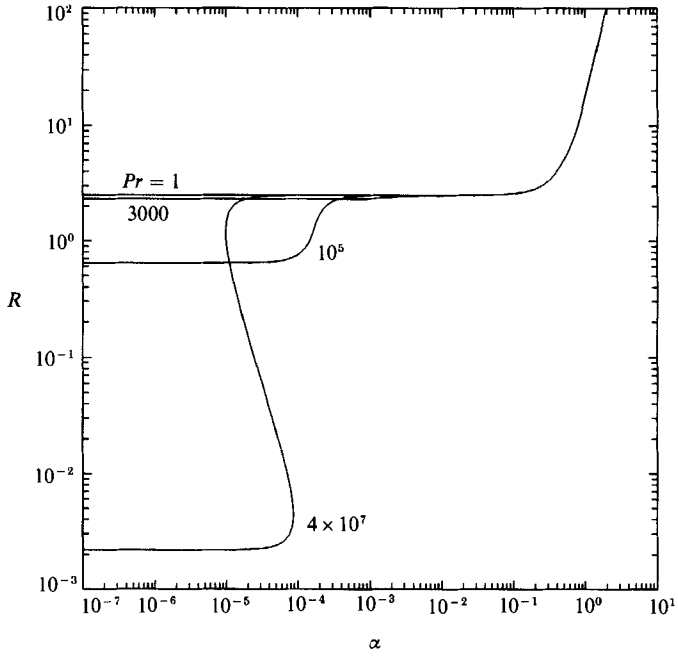

FIGURE 5. Neutral curves of the Reynolds number R versus the wavenumber α for different values of the Prandtl number Pr. The system is stable below the curves and unstable above. The layer is heated from below and has an isothermal top surface. Other parameter values are $E = -10^{-3}$, $B = \infty$, $Ca = \infty$ and $\beta = 45°$.

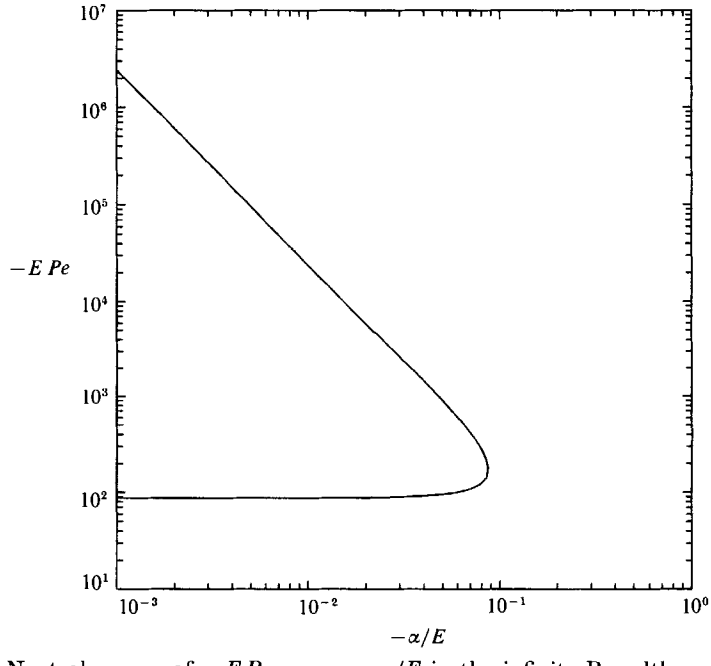

FIGURE 6. Neutral curves of $-E\,Pe$ versus $-\alpha/E$ in the infinite-Prandtl-number limit for three values of the expansion number, $E = -10^{-4}$, -10^{-3} and -10^{-2}. The system is stable outside the region bounded by the curve and the vertical axis and unstable inside. The layer is heated from below and has an isothermal top surface. Other parameter values are $B = \infty$, $Ca = \infty$ and $\beta = 45°$. All three curves are indistinguishable on this plot.

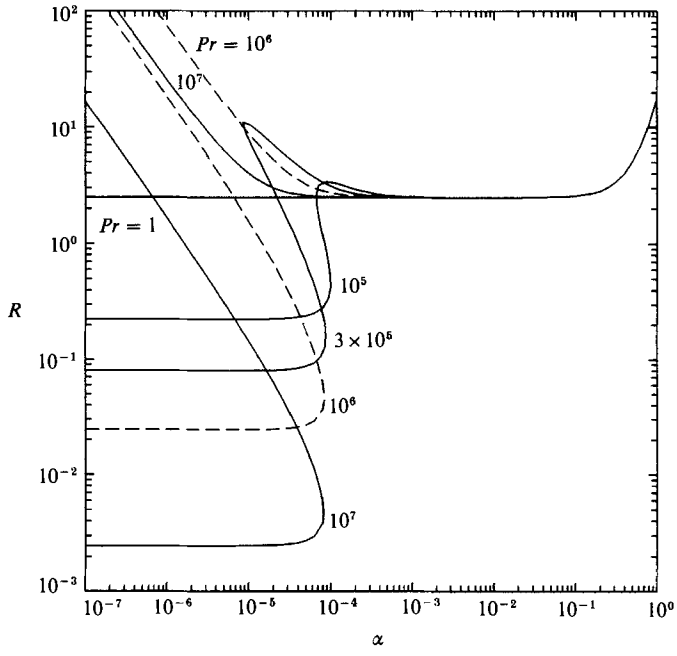

FIGURE 7. Neutral curves of the Reynolds number R versus the wavenumber α for different values of the Prandtl number Pr. When the neutral curve is a single curve, the system is stable below the curve and unstable above. When the neutral curve is two separate curves, the system is stable outside the region bounded by the lower curve and the vertical axis, and it is unstable inside this region. The system is also unstable above the upper curve. The layer is cooled from below and has an insulated top surface. Other parameter values are $E = 10^{-3}$, $B = 0$, $Ca = \infty$ and $\beta = 45°$.

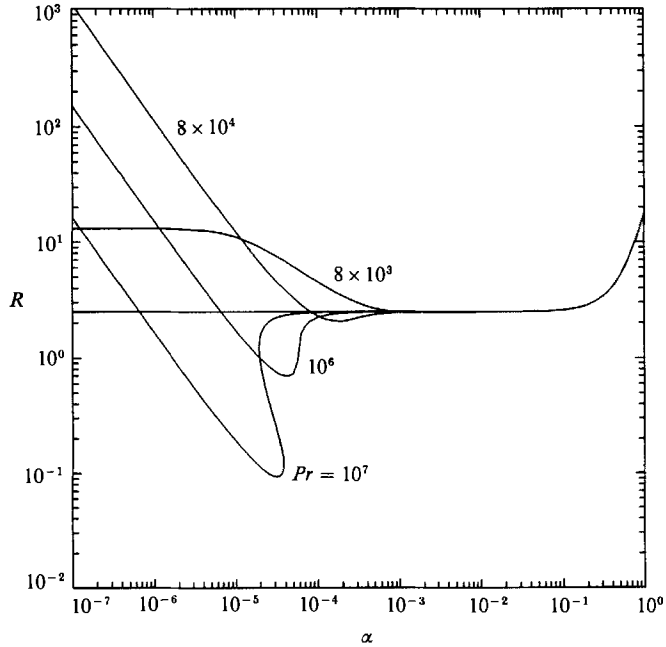

FIGURE 8. Neutral curves of the Reynolds number R versus the wavenumber α for different values of the Prandtl number Pr. The system is stable below the curves and unstable above. The layer is heated from below and has an insulated top surface. Other parameter values are $E = -10^{-3}$, $B = 0$, $Ca = \infty$ and $\beta = 45°$.

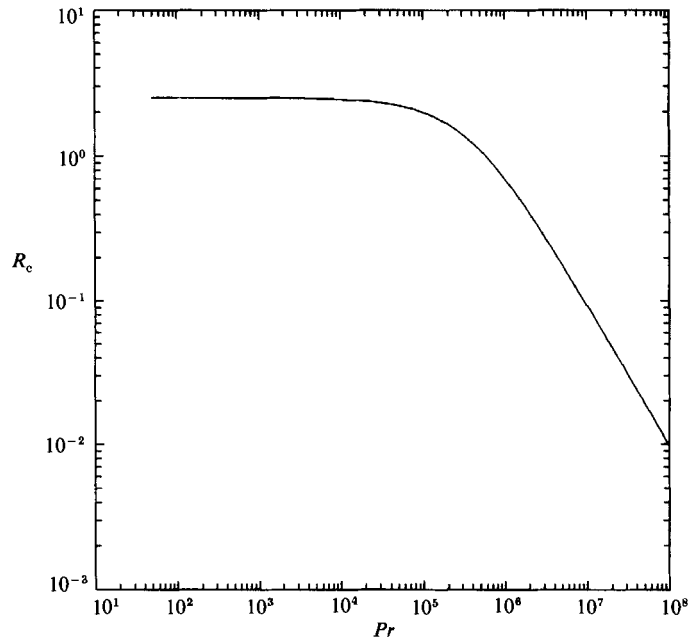

FIGURE 9. The value of the critical Reynolds number R_c versus the Prandtl number Pr for the neutral curves of figure 8. The layer is heated from below and has an insulated top surface. Other parameter values are $E = -10^{-3}$, $B = 0$, $Ca = \infty$ and $\beta = 45°$.

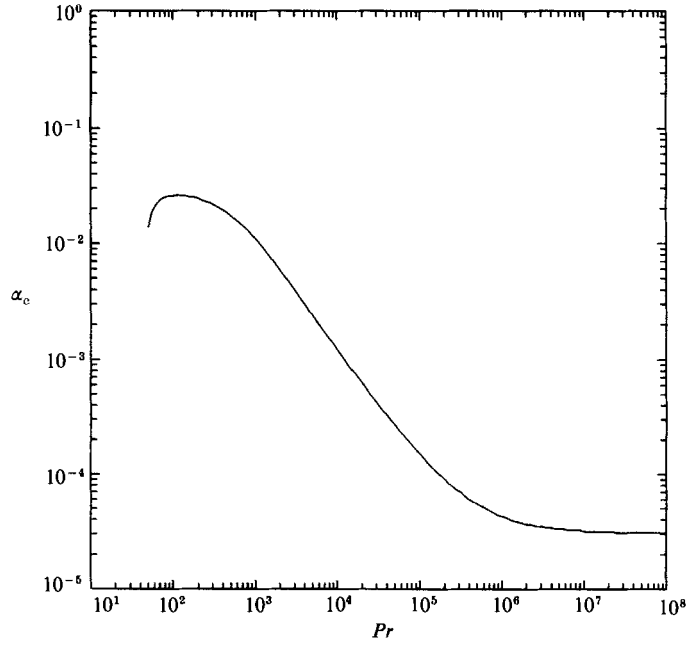

FIGURE 10. The value of the critical wavenumber α_c versus the Prandtl number Pr for the neutral curves of figure 8. The layer is heated from below and has an insulated top surface. Other parameter values are $E = -10^{-3}$, $B = 0$, $Ca = \infty$ and $\beta = 45°$.

again as predicted in the analysis of §2. However, the behaviour of the critical point of these neutral curves is markedly different than those of the cooled layer with an isothermal top surface shown in figure 4. In figure 4, the critical points are contained near and above the neutral curve for the isothermal case. In figure 8, the critical point moves below the isothermal neutral curve as Pr gets large. The critical Reynolds number and the critical wavenumber as a function of Pr are shown in figures 9 and 10 respectively. These curves start at $Pr = 50$, because for $Pr < 50$ the critical point lies at $\alpha = 0$. As Pr gets large, $R_c \sim Pr^{-1}$ and the critical wavenumber approaches a constant value.

The results of this section are summarized as follows. The critical points for a heated layer with an isothermal top surface and a cooled layer with an insulating top surface occur at $\alpha = 0$. The critical Reynolds number can be calculated from (2.13*c*) up to $O(E^2)$. For a cooled layer with an isothermal top surface, the instability has a finite, but small, wavelength. The critical Reynolds number is always near the value for an isothermal layer. When the layer is heated with an insulating top surface, the instability also has a small but finite wavelength, as shown in figure 10. However, the critical Reynolds number decreases from its isothermal value as the Prandtl number increases (figure 9).

5. Discussion

Our results show that thermal conditions can influence the stability of an inclined liquid layer to long waves. When $|EPr| > 4$, heating or cooling the layer changes the critical Reynolds number by 10% or more for any value of the Biot number. Using a typical value for the expansion coefficient $\gamma = 10^{-3}\ ^\circ\mathrm{C}^{-1}$ and a $\Delta T = 4\ ^\circ\mathrm{C}$, this threshold corresponds to $Pr > 1000$. Thus, only fluids with large Prandtl numbers exhibit this effect. Goussis & Kelly (1982) argued that all $O(E)$ terms are negligible when E is small. Their arguments are valid for moderate and small values of the Prandtl number, but they fail when the Prandtl number is large because they neglected the effect of the Prandtl number on the temperature distribution in the layer.

When an inclined liquid layer is heated from below, it can become unstable to both long waves and to Rayleigh–Bénard convection. It is best to relate these two instabilities by considering the Rayleigh number, defined as $Ra = -gd^3\gamma\Delta T/\nu\kappa$, where Ra is positive for heating from below. Noting the relation

$$Ra = -RE\,Pr/\sin(\beta),$$

equation (2.12*c*) for the layer with an isothermal top surface becomes

$$Ra_c = -\frac{5}{2}\frac{\cot(\beta)}{\sin(\beta)} EPr\left\{1 - \frac{11}{384}EPr\right\}^{-1}. \tag{5.1}$$

Kelly & Goussis (1982) found that the preferred mode of thermal convection on a rigid inclined plane takes the form of longitudinal rolls and so the critical Rayleigh number is

$$Ra_c = \frac{Ra_0}{\cos(\beta)}, \tag{5.2}$$

as found by Kirchgässner (1962). Here, $Ra_0 = 1100$ is the critical Rayleigh number for a horizontal layer with a free isothermal upper surface and a rigid isothermal

lower surface (Chandrasekhar 1961), and the $\cos(\beta)$ in the denominator reflects the decrease in the normal component of gravity as the inclination angle of the rigid plate is increased. This result does not depend on the parameters EPr because this is a steady mode of convection and it is easy to show that the critical Rayleigh number is independent of the Prandtl number.

Comparing these two results, we find that the critical Rayleigh number for the long-wave instability is less than that of the convective instability when the angle of inclination of the plate is greater than a transition angle β_l given by

$$\tan^2(\beta_l) = -\frac{5EPr}{2Ra_0}\left\{1-\frac{11}{384}EPr\right\}^{-1}. \tag{5.3}$$

Thus, long waves are seen first when $\beta > \beta_l$ and longitudinal rolls are seen first when $\beta < \beta_l$. Note that (5.3) reduces to the result of Kelly & Goussis (1982) when EPr is small. As an example, consider the silicone oil AK350 and a temperature differential across the layer of 5 °C. Long waves appear first when $\beta > 9.7°$. If thermal effects on the long-wave instability were ignored, we would predict long waves for $\beta > 12.1°$.

Thermal effects in a heated or cooled inclined liquid layer influence the behaviour of the long-wave instability in two different ways. The first way is to induce longitudinal buoyancy forces that drive additional motion in the layer. The second is through direct expansion of the liquid. The process through which these thermal effects influence the instability can be understood in terms of an extension to the physical mechanism for the long-wave instability of an inclined isothermal liquid layer given by Smith (1990). The first two terms of c_1 given in (2.11*b*) represent the net effects of this isothermal instability mechanism. The first term measures the destabilizing effect of inertia in response to a disturbance of the viscous flow in the layer. The $\cot(\beta)$ term represents the stabilizing effect of the hydrostatic pressure in the layer.

To describe the instability mechanism due to thermal effects, consider a long-wave disturbance to the interface of an inclined liquid layer that is cooled from below, as shown in figure 11. (The arguments for the case of a layer heated from below are similar.) In the cooled layer, the basic-state temperature increases linearly upward. When the position of the interface is deflected upwards by a disturbance, the basic-state temperature at the new location is larger than at the undisturbed location (see figure 11*a*). If the interface is *isothermal*, a negative temperature perturbation must develop there that balances the increase in temperature due to the basic state. Thus, a cold spot develops at the disturbance crest. Likewise, at a depression of the interface, a hot spot develops in order to maintain the temperature of the interface at a constant temperature. This effect is readily seen in the thermal boundary condition at the free surface (2.4*i*) when $B \to \infty$. The leading-order disturbance temperature field that results is shown in figure 11(*b*). It is linear because it is dominated by heat conduction normal to the layer.

The next correction to the temperature field is of $O(\alpha)$ and is governed by (2.8*d*). We see that heat advection modifies the conduction temperature field in two ways. The dominant one is the advection of the leading-order temperature disturbance by the basic-state velocity relative to the moving disturbance. Because the phase speed of the disturbance is positive and larger than the basic-state velocity at any point within the layer, the horizontal motion of the fluid with respect to the disturbance will always be in the upstream direction. In figure 12(*a*), we see that to the left of a disturbance crest, the horizontal motion of the fluid advects cooler fluid particles

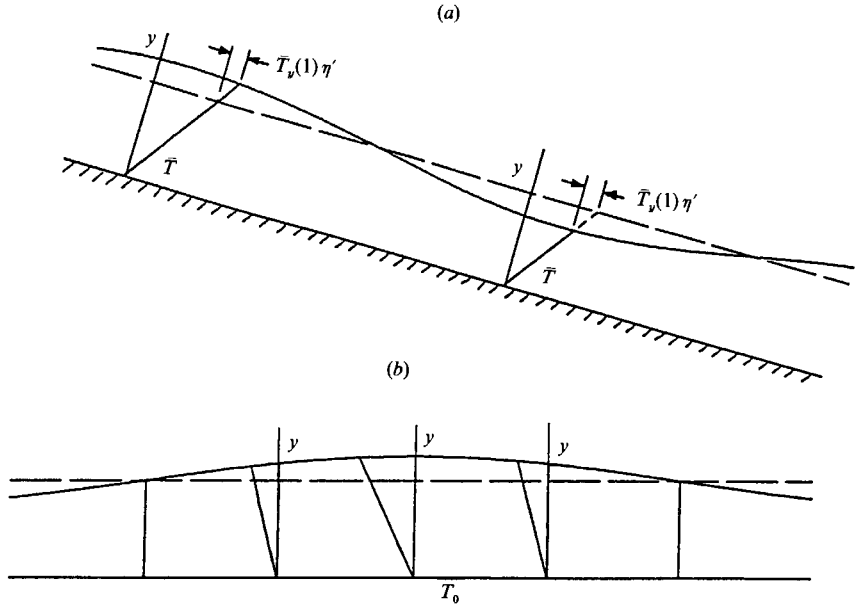

FIGURE 11. The development of the leading-order temperature perturbation in a liquid layer with an isothermal top surface when it is cooled from below. (*a*) The change in the basic-state interfacial temperature due to a long-wave deformation of the interface, and (*b*) the resulting leading-order temperature perturbation. The long-dash line is the undisturbed free-surface position.

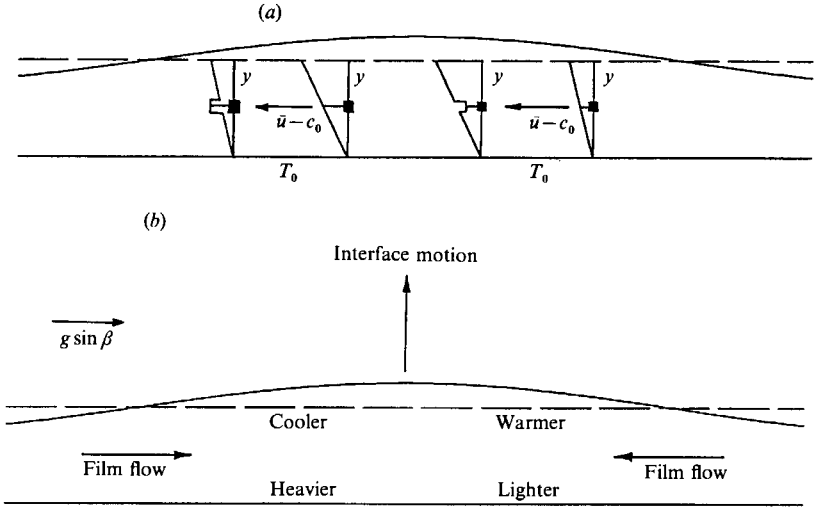

FIGURE 12. A schematic of the heat advection effect in the liquid layer. (*a*) The advection of fluid at the leading-order temperature by the basic-state velocity relative to the moving disturbance, and (*b*) the first-order temperature perturbations produced by the advection shown in (*a*) and the film flow and the induced interfacial motion produced by the buoyancy force acting in the longitudinal direction. The long-dash line is the undisturbed free-surface position.

from near the crest to the warmer regions of the layer near the node point. This has a cooling effect on the fluid to the left of the crest. Similarly, to the right of the crest, horizontal motion advects warmer fluid from near the node point towards the cooler fluid near the crest. This has a heating effect on the fluid to the right of the crest. The magnitude of this advection effect is measured by the Prandtl number. If Pr is small,

heat diffusion dominates and advection effects are not noticeable. However, for large Prandtl numbers, heat advection is important and the temperature distribution in the layer is significantly modified. Specifically, the temperature decreases to the left of the crest and increases to the right.

We note that this advection process is composed of advection by the horizontal basic-state velocity and an unsteady term due to the motion of the disturbance. The unsteady term has the larger effect. Thus, we can describe the modification of the temperature field in another way. Consider a disturbance to the interface and a fixed point in the layer just ahead of the crest of the disturbance. As the disturbance moves over the fixed point, the temperature in the layer must decrease in order to follow the conduction-dominated temperature solution. However, the heat capacity of the liquid represented by the unsteady term prevents the fluid temperature at this point from decreasing fast enough. Thus, the temperature of the fluid in front of the crest of the disturbance is slightly higher than the conductive solution would indicate. Likewise, just behind the crest, the opposite happens and the temperature is slightly cooler than expected.

Now consider the effect of this modified temperature distribution on the buoyancy forces in the layer. To the left of the crest the fluid is colder and therefore more dense than before. It will tend to move downstream under the longitudinal component of gravity, $g\sin(\beta)$. Just to the right of the crest, the fluid is warmer and therefore less dense than before so it tends to move upstream. The net result is a flow of fluid towards the crest and away from the troughs of the disturbance as indicated in figure 12(*b*). A simple conservation-of-mass analysis then shows that the deflection of the interface must increase. Thus, longitudinal buoyancy has a destabilizing effect.

The influence of this temperature field is also felt through the direct expansion of the liquid as described in (2.10*d*). When the disturbance moves over a fixed point in the layer, the temperature field decreases continually from the node point in front of the disturbance crest to the node point behind. A temperature decrease causes the fluid to contract. The response of the interface is a decrease in the elevation of the disturbance. In fact, this stabilizing effect dominates the destabilizing effect of longitudinal buoyancy and so cooling a liquid layer with an isothermal top surface from below is stabilizing to long waves.

When the top surface of the layer is insulated, a disturbance to the interface has no leading-order effect on the temperature field; see (2.7*a*). Since the basic-state heat flux through the layer must remain fixed, the temperature in the bulk of the layer does not change when the interface is deformed. With $T_0 = 0$ in this case, the dominant advection term in (2.8*d*) is due to the normal velocity disturbance in the layer. The mechanism for its effect is shown in figure 13. To the left of the disturbance crest the normal disturbance velocity in the layer is in the $-y$-direction. It advects fluid with a higher basic-state temperature to regions where it is colder. This has a heating effect on the fluid and so the temperature of the layer to the left of the crest is increased. Likewise, the normal disturbance velocity to the right of the disturbance crest has a cooling effect and the temperature there is lowered. This temperature perturbation modifies the density of the fluid so that longitudinal buoyancy produces a stabilizing flow away from the disturbance crest as shown in figure 13(*b*). As the disturbance moves over a fixed point in the layer, the disturbance temperature is such that the temperature increases from the node point in front of the crest to the node point behind the crest. The temperature increase directly expands the liquid and results in an increase in the deflection of the interface. This destabilizing effect dominates the stabilizing effect of longitudinal buoyancy and so the long-wave

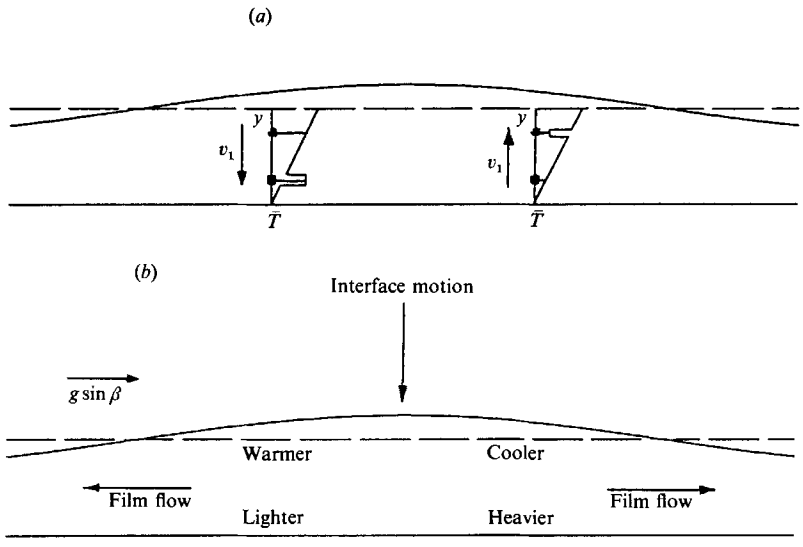

FIGURE 13. A schematic of the heat advection effect in the liquid layer. (*a*) The advection of fluid at the basic-state temperature by the normal perturbation velocity, and (*b*) the first-order temperature perturbations produced by the advection shown in (*a*) and the film flow and the induced interfacial motion produced by the buoyancy force acting in the longitudinal direction. The long-dash line is the undisturbed free-surface position.

instability of a liquid layer with an insulated top surface is further destabilizing by cooling from below.

The relative effects of all the processes discussed above can be shown by considering the thermal term in the imaginary part of the eigenvalue given by (2.11*b*). For an isothermal top surface ($\mathscr{B} = 1$), this thermal term is

$$-\mathrm{i}EPe\frac{11}{2880} = \mathrm{i}EPe\left\{\frac{5}{1152} - \frac{47}{5760}\right\}. \tag{5.4}$$

The first term on the right-hand side is the destabilizing effect of longitudinal buoyancy forces and the second is the stabilizing effect of direct liquid expansion. In the buoyancy term, we have

$$\mathrm{i}EPe\frac{5}{1152} = \mathrm{i}EPe\left\{\frac{73}{8064} - \frac{19}{4032}\right\}. \tag{5.5}$$

The first term on the right-hand side is the contribution to the destabilizing effect of longitudinal buoyancy from longitudinal advection in the T_1-disturbance equation and the second term is the stabilizing contribution from normal advection. Likewise for the expansion term,

$$-\mathrm{i}EPe\frac{47}{5760} = \mathrm{i}EPe\left\{-\frac{643}{40320} + \frac{157}{20160}\right\}. \tag{5.6}$$

Considering the expansion term differently, we find

$$-\mathrm{i}EPe\frac{47}{5760} = \mathrm{i}EPe\left\{-\frac{1}{80} + \frac{5}{1152}\right\}. \tag{5.7}$$

The first term on the right-hand side is the contribution to the stabilizing effect of direct liquid expansion due to unsteady effects as the T_1-temperature field moves

downstream with the disturbance. The second term is the destabilizing contribution from horizontal advection of the density in the liquid as modified by the T_1-temperature field.

For an insulated top surface ($\mathscr{B} = 0$), the thermal term in the imaginary part of the eigenvalue is

$$\mathrm{i}EPe\frac{17}{1260} = \mathrm{i}EPe\left\{-\frac{31}{1008}+\frac{223}{5040}\right\}. \tag{5.8}$$

The first term on the right-hand side is the stabilizing effect of buoyancy forces and the second is the destabilizing effect of direct liquid expansion. Both of these effects arise from a temperature field caused by normal advection of the fluid since there is no $O(1)$ temperature perturbation to be advected by the horizontal motion in the layer. Considering the expansion term, we find

$$\mathrm{i}EPe\frac{223}{5040} = \mathrm{i}EPe\left\{\frac{3}{40}-\frac{31}{1008}\right\}. \tag{5.9}$$

The first term on the right-hand side is the contribution to the destabilizing effect of direct liquid expansion due to unsteady effects as the T_1-temperature field moves downstream with the disturbance. The second term is the stabilizing contribution from horizontal advection of the density in the liquid as modified by the T_1-temperature field.

Our discussion up to this point has centred on the forces that drive the flows responsible for the unstable motion of the interface. It is also appropriate to comment on how the energy for the instability is fed to the long-wave disturbance. The sources of disturbance energy in this problem can be found by using a disturbance energy analysis as shown by Kelly *et al.* (1989) for the isothermal liquid layer. A full analysis of this kind is rather complex and will not be discussed in this work. However, we have noted that the thermal part of the long-wave instability is seen in the layer even when the Reynolds number is zero, as shown in (3.4). In this limit, a disturbance energy analysis shows that the rate of increase in the disturbance energy is due to the increase in thermal energy alone. The rate of increase in thermal energy can be obtained by multiplying the disturbance energy equation by T' and integrating over the depth of the layer and over one wavelength λ of the disturbance. The resulting equation for a layer with the isothermal top surface is

$$\frac{\mathrm{d}\mathscr{E}}{\mathrm{d}t} = -\int_V \bar{\rho}\bar{T}_y\, v'T' - Pe^{-1}\int_0^\lambda \bar{T}_y(1)\, T'_y(y=1)\,\eta'\,\mathrm{d}x - \mathscr{D}, \tag{5.10}$$

where $\mathscr{E} = \int_V(\frac{1}{2}\bar{\rho}T'^2)$ is the total thermal energy of the disturbance, $\mathscr{D} = Pe^{-1}\int_V(T'^2_x + T'^2_y)$ is the amount of thermal energy dissipation, and $\int_V$ is the required volume integral.

The first two terms on the right-hand side of (5.10) measure the production of disturbance energy. The first term represents the transfer of thermal energy from the basic-state temperature field to the disturbance through advection by the normal velocity in the layer. The second term shows how energy is transferred to the disturbance through a perturbation heat flux that develops at the interface due to its deformation and the presence of a basic-state heat flux. We can easily see that the first energy production term is $O(\alpha)$ in the long-wave limit, and that the second is $O(1)$. Thus, the perturbation heat flux at the interface is the primary source of disturbance energy for the long-wave instability in a liquid layer with an isothermal top surface. When the top surface is insulating, the second production term is zero

and so the only process that delivers energy to any disturbance is advection by the normal velocity in the liquid layer. In both cases, the energy reservoir for the disturbance is the thermal energy contained in the basic-state thermal field.

6. Conclusions

We have examined the effect of heating or cooling on the interfacial long-wave instability of a liquid layer flowing down a rigid inclined plane. The growth rate of long-wave disturbances αc_i is the result of three distinct effects as shown in (2.11*b*). The first two terms in this equation are the imaginary part of the eigenvalue for an isothermal liquid layer and were first derived by Benjamin (1957) and Yih (1963). The first term is the destabilizing effect of the inertia of the liquid on the disturbed viscous flow in the layer as explained by Smith (1990). The second term represents the stabilizing effect of the hydrostatic pressure in the layer as it increases with the interfacial deformation.

The contribution of the present work has been to identify and explain the third term in (2.11*b*). This term is composed of contributions from longitudinal buoyancy forces and from direct liquid expansion effects. It is measured by the expansion number E, which is usually small. Previous work on this problem has usually either ignored or neglected these effects because of this. However, we have shown that these effects are truly negligible only when EPr is small. In this case, the stability of a heated or cooled liquid layer to long waves is essentially the same as an isothermal layer. However, when $EPr = O(1)$, i.e. for large-Prandtl-number fluids, these effects are not negligible because advection will modify the temperature distribution enough for buoyancy and expansion effects to appear.

The behaviour of the layer as a result of these thermal effects is somewhat surprising. When the top surface is almost isothermal, cooling the layer from below is stabilizing to long waves and heating from below is destabilizing. This is the behaviour one might expect. However, when the top surface is almost insulating, cooling the layer from below is destabilizing to long waves and heating from below is stabilizing.

When the layer is stabilized to long waves, an analysis of the system at finite wavenumbers is needed in order to predict the critical mode of instability in the layer. The results of this analysis showed that long waves are preferred when the layer is heated from below with an almost isothermal top surface and when it is cooled from below with an almost insulating top surface. The critical wavenumber for a layer cooled from below with an almost isothermal top surface is finite, but still small. The critical Reynolds number is only different from the isothermal result by an $O(E)$ amount. The critical wavenumber for a layer heated from below with an almost insulating top surface is also finite and small. However, the critical Reynolds number can be much less than that of the isothermal layer. In fact as $Pr \to \infty$, $R_c \sim Pr^{-1}$.

The physical mechanisms for the effect of longitudinal buoyancy and of direct liquid expansion on long waves were explained using arguments similar to those described by Smith (1990) for the isothermal problem. Consider a liquid layer that is cooled from below and whose top surface is almost isothermal. The temperature of the liquid in this layer is determined mainly by conduction. If the interface is deformed by a long-wave disturbance, the temperature in the bulk of the liquid decreases as the thickness of the layer increases. The disturbance propagates downstream just as in the isothermal case, and when the deflection of the interface

increases over a point in the layer, the temperature in the bulk of the layer should decrease. However, the heat capacity of the fluid prevents it from changing temperature as fast as the interface changes height. The result is that the temperature downstream of the crest of the disturbance is slightly higher than expected from conduction alone, while upstream of the crest of the disturbance it is slightly lower than expected. The longitudinal buoyancy force acts on the slightly warmer fluid downstream of the crest and drives a flow towards the crest of the disturbance. Upstream of the crest, buoyancy acts on the slightly colder fluid and also drives a flow towards the crest of the disturbance. The effect of these two flows is destabilizing since they tend to increase the deflection of the interface.

The effect of direct liquid expansion is also felt through the action of this slightly perturbed temperature field. As the disturbance moves over a fixed point in the layer, the perturbation of the conduction temperature field is seen as a continual decrease in the temperature as the crest of the disturbance moves by. This decrease in temperature decreases the volume of the liquid which stabilizes the disturbance because it tends to decrease the deflection of the interface. This effect is larger than the destabilizing effect of buoyancy and so the overall influence of cooling is stabilizing.

If we consider the top surface of the layer to be insulating, then the temperature field in the layer is less affected by a disturbance in the thickness of the layer because the slope of the temperature profile in the layer must remain constant. However, as a disturbance crest moves along the interface, there is a slight normal motion in the bulk liquid that is towards the interface downstream of the crest and away from the interface upstream of the crest. As the fluid in the layer moves towards the interface, it brings colder fluid from below towards the surface. This has a cooling effect and so the fluid downstream of the disturbance crest is slightly colder than expected from conduction alone. Likewise, the fluid upstream of the crest brings hotter fluid from near the surface down into the colder fluid near the bottom and so the temperature upstream of the crest is slightly hotter than expected from conduction alone. Longitudinal buoyancy forces and direct liquid expansion then act on this perturbed temperature field to produce a stabilizing and a destabilizing flow perturbation respectively. The direct expansion effect is greater and so cooling from below is destabilizing when the top surface is insulating.

The physical mechanisms that we have described in this work also explain why the thermal effects of heating or cooling influence the long-wave instability of a liquid layer only when the liquid has a large Prandtl number. These thermal effects are the result of temperature changes in the layer, due to unsteadiness or normal advection, that are proportional to the Prandtl number. These temperature changes then produce small changes in the liquid's buoyancy that are proportional to the expansion number. Since the expansion number is small, thermal effects are important only when the Prandtl number is large.

Earlier research on this problem has either neglected or ignored longitudinal buoyancy because of the smallness of the expansion number. Recently, Yih (1986) considered the flow in an inclined channel containing two liquid layers that have different thermal conductivities, but in which all other fluid properties are identical. When the channel is cooled from below and heated from above, a long-wave instability of the interface between the liquids is possible when the less conductive liquid is above the more conductive liquid. Yih says that the driving force for this instability is longitudinal buoyancy and that this force is produced because of temperature perturbations caused by the difference in the thermal conductivities of

the two liquids. A careful examination of Yih's analysis shows that the basic mechanism for his instability is the same as the mechanism for longitudinal buoyancy effects that we have described in this work. Thus, a multilayered system with thermal conductivity stratification is not the only system that displays this kind of long-wave instability.

There is also a close similarity between the major source of thermal disturbance energy production for the interfacial instability in a stratified channel and in a single liquid layer with an isothermal top surface. In each case, energy is transferred from the basic-state temperature field to the long-wave disturbance through a perturbation heat flux that develops at the interface. The processes that form the perturbation heat flux are slightly different, however, because different thermal boundary conditions are used on the interface in each system.

There are two other differences between the interfacial instability in the single liquid layer and in the two-layer channel flow. First, the basic state in the channel flow does not have a jump in the curvature of the basic-state velocity profile at the interface. Therefore, an interfacial deformation does not induce a disturbance shear stress on the interface as it does for the flow in a single liquid layer on an inclined plane. The basic-state velocity and the leading-order velocity disturbance in the channel flow are due to the small longitudinal buoyancy effects that are negligible in the single liquid layer. Second, there is a lubrication pressure that appears in the channel flow system because of its confined geometry. Smith (1989) describes this pressure as it appears in a vertical, density-stratified, two-phase pipe flow. In fact, the lubrication pressure is responsible for the very complicated behaviour of the instability in the pipe flow problem as the thickness of the two fluids change. Thus, we should expect the behaviour of the instability in the channel flow system to become even more complicated as the two layers change in thickness.

Smith (1990) proposed that the interfacial long-wave instability seen in single inclined isothermal liquid layers and in multiple inclined liquid layers with stratification in density or viscosity could be classified into two large groups. The basic mechanism of the instability for each group was then studied using an appropriate single-layer model. In this same spirit, we note the similarities between the instability mechanism and the disturbance energy production mechanism in both the single-layer flow and the channel flow of Yih (1986). Therefore, the single-layer model presented in this paper seems to be the simplest system that exhibits all of the basic effects of heating and cooling on the long-wave instability.

One further comment on Yih's (1986) work is in order. We have shown that the thermal component of the long-wave instability in a single, inclined liquid layer is primarily the result of unstable fluid motions caused by direct liquid expansion. The longitudinal buoyancy forces that appear in the layer always oppose these motions. When Yih posed the two-layer channel flow problem, he used the incompressible form of the conservation of mass equation, and so he neglected the direct expansion of the liquid. If the present work is any guide, one should expect significantly different results in the channel flow when these direct liquid expansion effects are included. Such an investigation remains for the future.

Finally, long-wave instabilities have been found by Renardy (1986) in a two-layer system stratified by thermal conductivity and by Benguria & Depassier (1987) in a layer with a free, isothermal lower surface and a free, insulated upper surface. The main difference with the present work is that the previous layers were horizontal. The mechanism for this instability must be due to the effects of gravity in the vertical direction, and so it is not the same instability as the one seen in this work or in the work of Yih (1986).

This work was supported by the National Science Foundation, Grant No. MSM-8451093. The figures in this paper were drawn with the help of the NCAR graphics system.

REFERENCES

BANKOFF, S. G. 1971 *Intl J. Heat Mass Transfer* **14**, 377.

BENGURIA, R. D. & DEPASSIER, M. C. 1987 *Phys. Fluids* **30**, 1678.

BENJAMIN, T. B. 1957 *J. Fluid Mech.* **2**, 554.

CHANDRASEKHAR, S. 1961 *Hydrodynamic and Hydromagnetic Stability*. Dover.

DEBRUIN, G. J. 1974 *J. Engng Maths* **8**, 259.

FLORYAN, J. M., DAVIS, S. H. & KELLY, R. E. 1987 *Phys. Fluids* **30**, 983.

GOUSSIS, D. & KELLY, R. E. 1985 *Phys. Fluids* **28**, 3207.

KELLY, R. E. & GOUSSIS, D. 1982 *Heat Transfer 1982 – Proc. 7th Intl Heat Transfer Conf.*, vol. 5, p. 319. Hemisphere.

KELLY, R. E., GOUSSIS, D. A., LIN, S. P. & HSU, F. K. 1989 *Phys. Fluids* A **1**, 819.

KIRCHGÄSSNER, K. 1962 *Ing. Arch.* **31**, 115.

LIN, S. P. 1975 *Lett. Heat Mass Transfer* **2**, 361.

MARSCHALL, E. & LEE, C. Y. 1973 *Intl J. Heat Mass Transfer* **16**, 41.

RENARDY, Y. 1986 *Phys. Fluids* **29**, 356.

ROCA, R. 1966 *J. Méc.* **5**, 117.

SCOTT, M. R. & WATTS, H. A. 1975 *Rep.* SAND75-0198, Sandia Labs, Albuquerque, NM.

SCOTT, M. R. & WATTS, H. A. 1977 *SIAM J. Numer. Anal.* **14**, 40.

SMITH, M. K. 1989 *Phys. Fluids* A **1**, 494.

SMITH, M. K. 1990 The mechanism for the long-wave instability in thin liquid films. *J. Fluid Mech.* (in press).

SREENIVASAN, S. & LIN, S. P. 1978 *Intl J. Heat Mass Transfer* **21**, 1517.

ÜNSAL, M. & THOMAS, W. C. 1978 *Trans. ASME* C: *J. Heat Transfer* **100**, 629.

YIH, C.-S. 1963 *Phys. Fluids* **6**, 321.

YIH, C.-S. 1986 *Phys. Fluids* **29**, 1769.